INFN - Laboratori Nazionali di Frascati
Servizio Documentazione

LNF-91/069(P)
28 ottobre 1991

SUPERCONDUCTING PROPERTIES OF $Nb_{.75}Zr_{.25}$-OXIDE-$Nb_{.75}Zr_{.25}$ TUNNEL JUNCTIONS

U. Gambardella, D. Di Gioacchino
INFN-Laboratori Nazionali di Frascati
P. O. box 13, 00044 RM Frascati, Roma, Italy

G. Paternò
ENEA-CRE Frascati
P. O. box 65, 00044 RM Frascati, Roma, Italy

M. Cirillo
Dipartimento di Fisica
Università di Roma Tor Vergata
00173 RM Roma, Italy

ABSTRACT

We have fabricated symmetrical $Nb_{.75}Zr_{.25}$/Oxide/$Nb_{.75}Zr_{.25}$ tunnel junctions having cross type geometry. The superconducting films constituting the electrodes of the junctions were obtained by RF magnetron sputtering and the tunnel barrier was grown by natural oxidization in air. From the current-voltage characteristics of the junctions we have measured the temperature dependence of the energy gap of $Nb_{.75}Zr_{.25}$ and compared this dependence with BCS-theory results. The magnetic field diffraction pattern of the Josephson current of the junctions allows us to evaluate the penetration depth of the superconducting films. We also estimate the surface impedance of the NbZr film by measuring the quality factor of the junctions. We discuss the results within the framework of the realization of superconducting tunnel devices and coatings for superconducting accelerating cavities.

Work partially supported by CNR under the Progetto Finalizzato "Superconductive and Cryogenic Tecnologies"

1 - INTRODUCTION

There exists growing interest in the fabrication of superconducting thin films to be used in microwave devices or as coating materials in RF superconducting accelerator cavities[1,2]. Among the materials which have received attention in these areas NbZr has been extensively studied for practical and fundamental physics-oriented purposes[3,4]. The $Nb_{1-x}Zr_x$ bulk system has a critical temperature[5] $T_c \approx 10.8$ K for x=0.25, and shows a weak dependence on the exact composition[6] which is important for device fabrication and reproducibility. A limited amount of data is available from NbZr thin films[6,7] fabricated by using different methods, i. e. co-sputtering from two cathodes or electron-beam evaporation; in these cases the measured critical temperatures T_c was below 9 K.

In order to explain the noticeable increase in the critical temperature of $Nb_{.75}Zr_{.25}$ with respect to the critical temperature of the two components, tunneling measurements on asymmetrical junctions (NbZr/Al/Al_2O_3/In or NbZr/Ox/Pb) were performed: these studies allowed a determination of the electron-phonon coupling factor[4] λ, and of the superconducting energy gap[3,8] Δ of the NbZr. So far, however, the data that have been reported are from tunnel junctions realized on thin NbZr foils. Unfortunately, in measurements of the energy gap in asymmetrical junctions having In or Pb as a counterelectrode there are limitations both in the high temperature range due to the low T_c of the counterelectrode, and in the low temperature range where the only significant gap variation is not due to the NbZr. The use of artificial barriers has been considered because of the poor insulating properties of the NbZr natural oxide. However, when using the NbZr as a coating material one deals with the surface effects underlying and resulting from NbZr oxide; thus, it is interesting to investigate its superconducting features in more realistic operating conditions.

In this work we report the fabrication of thin $Nb_{.75}Zr_{.25}$/Ox/$Nb_{.75}Zr_{.25}$ film tunnel junctions realized by means of RF magnetron sputtering. The paper is structured as follows: in the next section we describe details of the fabrication process. In sect. 3 we present the results of direct $\Delta(T)$ measurements in the temperature range 8.5÷2.2 K ; the $\Delta(T)$ behavior is compared with theoretical BCS results. In sect. 4 we discuss the microwave properties of the NbZr film as estimated from the Josephson self-resonances of the junctions (our junctions exhibit indeed Josephson effect). The estimate of the surface impedance is compared with previous data obtained for a $Nb_{.75}Zr_{.25}$ film measured in a cylindrical TE cavity[9].

2 - FABRICATION OF THE JUNCTIONS

The films were RF magnetron sputtered on Corning glass 7059 or sapphire substrates. The cathode was a 3" diameter melted $Nb_{.75}Zr_{.25}$ disc. Aided by a LN_2 cold trap the vacuum prior to deposition of the films was in the range (2-4) x 10^{-7} mbar. The sputtering was performed in 5 x 10^{-3} mbar of Ar. Before each deposition, we pre-sputtered on a movable shield for 20 minutes. The pre-sputtering was carried out both to clean the target surface and to take benefit from the NbZr gettering action in the vacuum chamber. While the cathode was water cooled during the sputtering, the temperature of the substrates was allowed to rise. The deposition rates were 10 Å/s and 13 Å/s respectively for RF power of 500 W and 700 W. The film thickness ranged between 3000 Å and 5000 Å

As shown in Fig. 1, the critical temperature of our NbZr films was not strongly affected by the deposition rate, except at very low rates. In Fig. 2 we show resistance vs temperature for a typical $Nb_{.75}Zr_{.25}$ film. The residual resistivity ratio is 1.4 and the behavior is clearly nonlinear. A measurement of the transition temperature T_c, obtained with a calibrated thermometer, is shown in the inset: zero resistance is persistent up to T=10.1 K. The critical temperature is lower than that reported for bulk samples, but it is well above data previously reported for films.

The cross-geometry of the tunnel junctions was defined by using different metallic masks for the two depositions. The films widths range from 100 to 200 μm. The lower electrodes were usually thinner than the upper ones in order to obtain a good overlapping of the films. The oxide barriers were grown on the lower films by keeping the samples at room temperature in air for approximatively 17 hours. The films forming the counterelectrode were deposited at both the deposition rates mentioned above but, the experiments showed that the highest power does not give rise to tunneling effects.

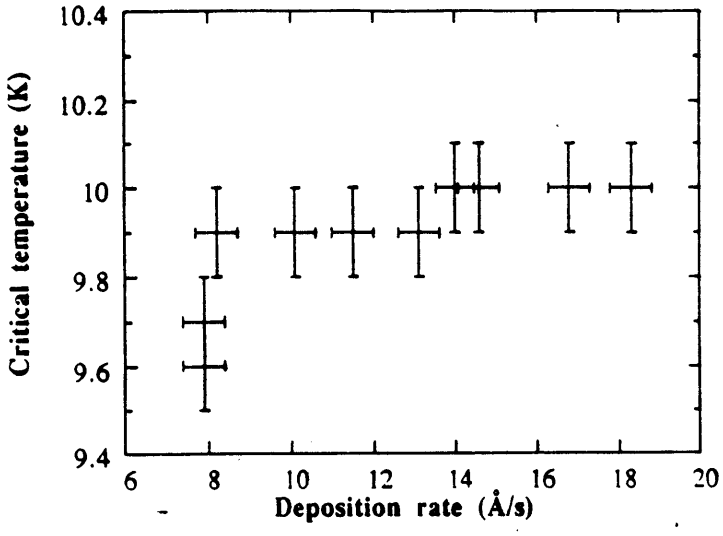

FIG. 1 - Critical temperature of $Nb_{.75}Zr_{.25}$ films as a function of the deposition rate.

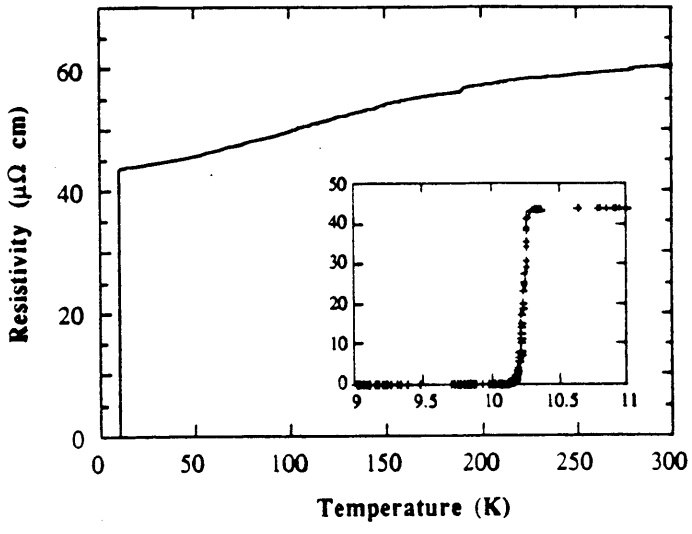

FIG. 2 - Typical R vs of $Nb_{.75}Zr_{.25}$ films. The inset shows the resistive transition.

3 - ENERGY GAP MEASUREMENTS

A preliminary scan of the tunneling features of our junctions was obtained with the sample in a LHe bath and using a 100 Hz triangular sweep current to display the current-voltage (I-V) characteristic on an oscilloscope. The junctions were connected in the usual four lead configuration. The I-V curves of the tunnel junctions were then recorded by biasing the junctions with a programmable current source and measuring the corresponding voltage by means of a high impedance differential nanovoltmeter. The measurements were performed by a computer which also stored the data. The temperature was measured by means of a calibrated carbon glass thermometer fed at constant current of 10 μA. In Fig. 3a a typical I-V characteristic at 4.2 K is plotted. The tunnel resistance above the gap voltage is $R_{NN} \approx 0.22\ \Omega$, but the sub-gap resistance exhibits a rather low value indicating the existence of a significant leakage current. The latter fact is very likely due to the existence of microshorts in the oxide barrier generated by the high deposition rate of the second electrode.

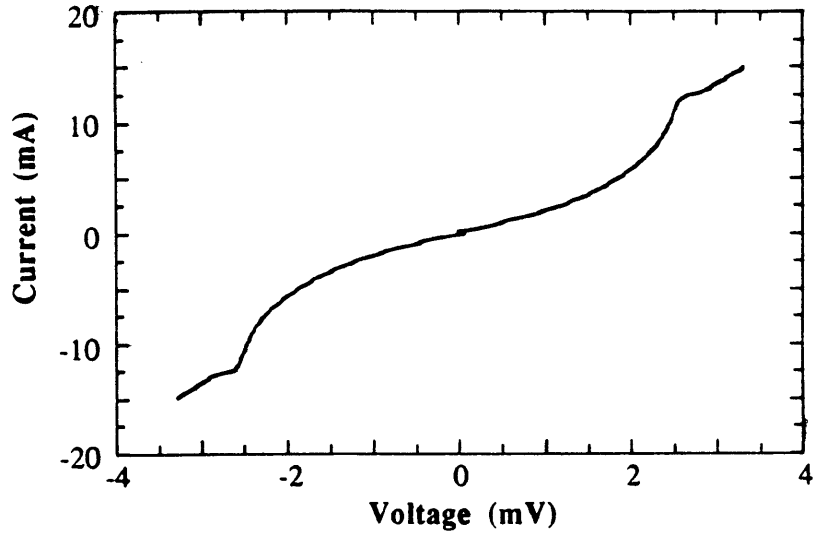

FIG. 3a - Typical I-V characteristic of NbZr-OxNbZr tunnel junction.

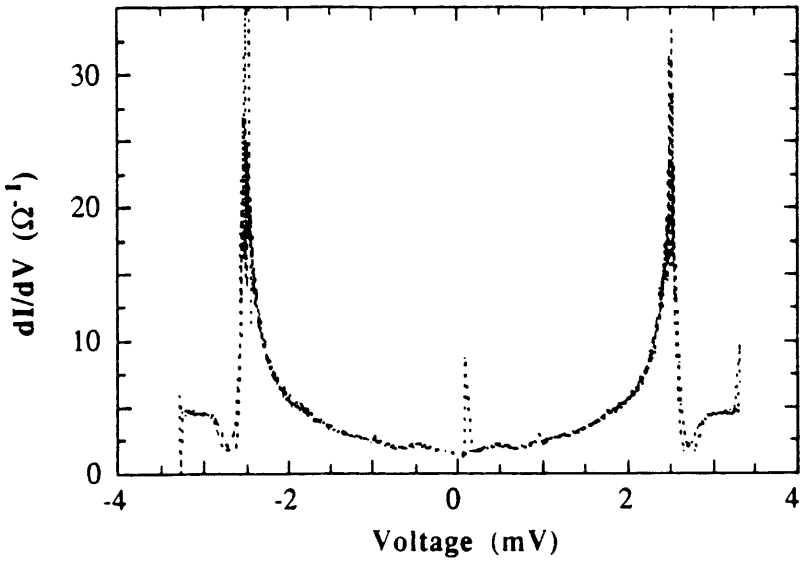

FIG. 3b - Typical dI/dV-vs-V characteristic.

The energy gap of a superconductor can be measured from the I-V characteristic of a tunnel junction[10,11]. This measurement can certainly be done with our junctions as the gap voltages are well defined. Temperatures above the LHe temperature were attained by keeping the sample in cold He vapour; we performed data acquisition only when the temperature was stable to within ±20 mK for several minutes. Furthermore, the temperature was checked at the beginning and at the end of the data acquisition, which lasted less than one minute. Temperatures lower than 4.2 K were obtained lowering the bath pressure. As usual, better resolution was achieved with the derivative of the curve, which was numerically computed and shown in Fig. 3b. The I-V curves of the junctions recorded at different temperatures were numerically processed to determine the corresponding energy gap voltage. As it is evident in Fig. 3a the I-V characteristics of our junctions exhibited a behavior indicating the presence of a proximity layer[12]. Thus we adopted the position of the second peak in the dI/dV-vs-V curves[4] as the gap voltage.

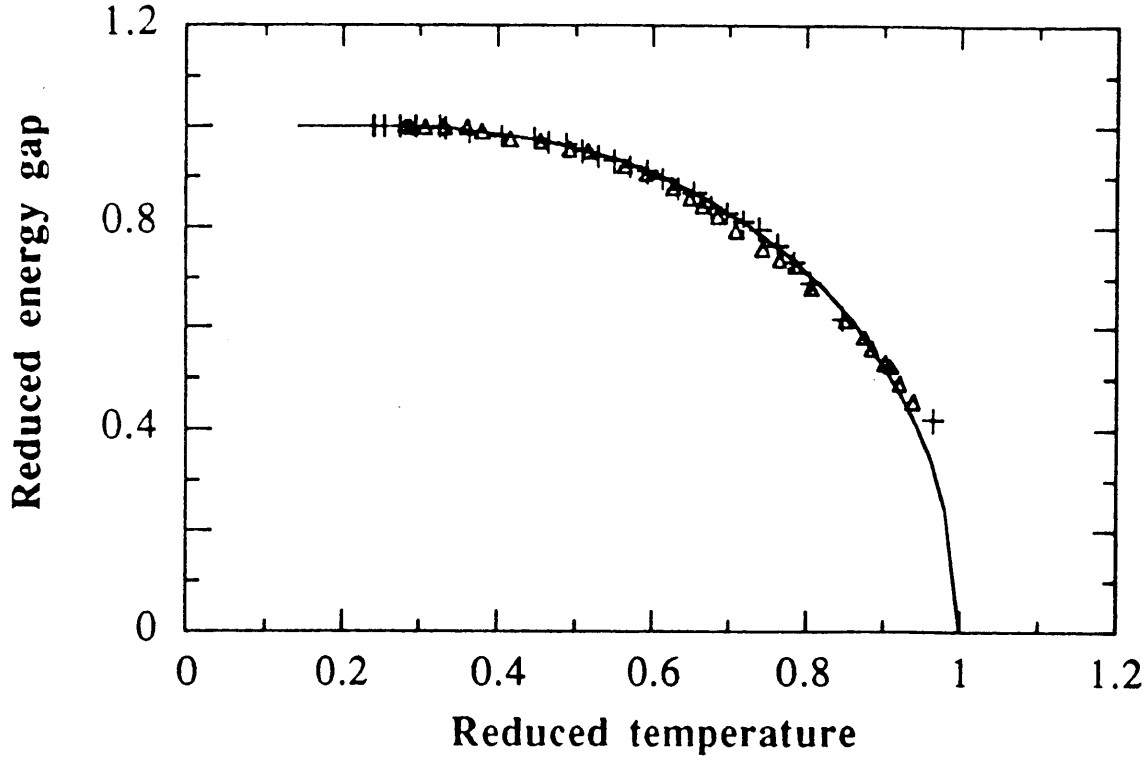

FIG. 4 - Reduced gap voltage as a function of the reduced temperature: (+) sample G8Ed, (Δ) sample G4Fd; solid line is the BCS theoretical behavior.

In Fig. 4 we show the reduced gap as a function of the reduced temperature for two samples. The normalizing coefficient $\Delta(0)$ for sample G8Ed (crosses) is the value measured at 2.28 K, i. e. $\Delta(2.28)=1.63$ mV, while the T_c used to normalize the temperature is $T_c=9.5$ K. On sample G4Fd (open triangles) we observed the same behavior but the data were reduced to $\Delta(2.43)\approx\Delta(0)=1.45$ mV and $T_c=8.5$ K. In Fig. 4 we also show the reduced BCS gap[13] (solid line). The agreement between the theory and experiment is satisfactory. The measured T_c of the junction electrodes is always higher than the T_c used to interpolate the data supporting the hypothesis of a surface layer having depressed superconducting parameters. In view of this

effect the "bulk" T_c is not significant for applications where the film surface is relevant. Assuming that the Fermi velocity v_F of Nb and $Nb_{.75}Zr_{.25}$ is similar[14] we estimate the intrinsic BCS coherence length of our films $\xi_0 = \hbar v_F / \pi \Delta(0)$ using the known values of Nb $\Delta_{Nb}(0)$=1.56 meV and $\xi_{0_{Nb}}$=430 Å. Thus, $\Delta(0)$=1.63 meV corresponds to $\xi_0 \approx 411$ Å. The corresponding value of $v_F \approx 3.1 \times 10^7$ cm/s leads to a mean free path $l=\tau v_F \approx 6.2$ Å, where $\tau \approx 2 \times 10^{-15}$ s is computed from the measured resistivity $\rho^{-1} = (1/4\pi)\, \omega_p^2 \tau$ and the reported plasma frequency[14] $(\hbar<\omega_p^2>)^{1/2} \approx 8$ eV.

4 - JOSEPHSON FEATURES

Some of the tunnel junctions that we fabricated exhibited the Josephson effect, which is useful to investigate superconducting features such as the magnetic penetration depth λ_{eff}. All the measurements on the Josephson junctions had to be performed in a magnetic shielded room, because of a very strong tendency to trap magnetic flux. The data were collected at 4.2 K keeping the sample in a LHe bath. We used the a.c. bias circuit to display the I-V curve and measured the maximum Josephson current from a voltage comparison provided by a different source. A magnetic field, perpendicular to the current flowing into the junction and parallel to the film surface, was provided by a long solenoid surrounding the junction. In Fig. 5 we show the behavior of the maximum Josephson current I_c as a function of the applied magnetic field for sample G4Fu (crosses). The zero-field current density was $J_{co} \approx 2.8$ A/cm^2, for junction dimensions of (LxW)=240x220 μm^2. The total penetration depth $d=2\lambda_{eff}+t$, where t is the oxide thickness, of the magnetic field in the junction can be calculated from the value of the field corresponding to the first minimum of the Josephson current $H^* = \phi_0/(Ld)$. We estimate $H^* \approx 0.4$ gauss from Fig. 5, so that $d \approx 2\lambda_{eff} \approx 2300$ Å.

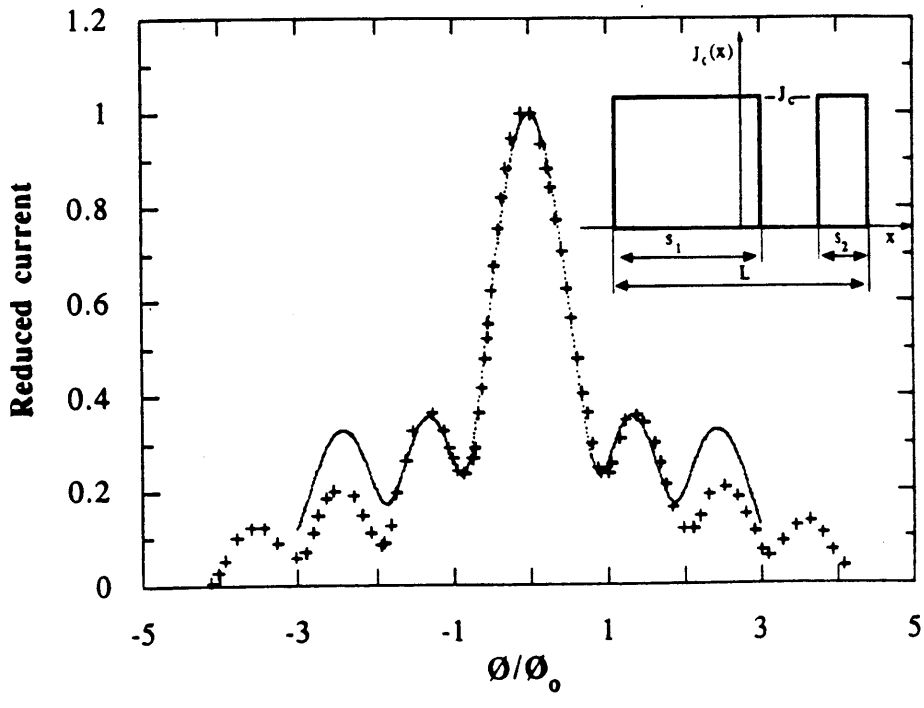

FIG. 5 - Maximum Josephson current as a function of the applied magnetic field for samples G4Fu. The solid line is the theoretical computation for an asymmetrical current distribution. The inset shows the model for the current distribution.

However, we realized from the non-zero current modulation that the current density is not uniform through the tunnel barrier. This behavior may be accounted for by using a model of asymmetric current density through the barrier[15]: in Fig. 5 we also show the theoretical behavior I(dotted line) of the Josephson current as a function of the reduced magnetic flux, for a junction having a length L where the current flows only through two regions s_1=0.58 L and s_2=0.20 L (see inset of Fig. 5). The agreement with experimental data is satisfactory, making our hypothesis realistic.

We compute the Josephson penetration depth from the relation[16]:

$$\lambda_J = \sqrt{\frac{h}{4\pi e\, \mu_o J_c}}$$

obtaining $\lambda_J \approx 320$ μm. From this result it comes out that this sample is a "small" junction, meaning that the Josephson penetration depth λ_J is larger than the cross junction length L, i. e. $L/\lambda_J < 1$. In Table I are listed typical quantities for some junctions which exhibited Josephson effect, such as the length L, the critical current density, the magnetic penetration depth λ_{eff} and the Josephson penetration depth λ_J.

TABLE I - Parameters for three Josephson tunnel junctions.

Sample	L (μm)	S (mm^2 x10^{-2})	J_c (A/cm^2)	λ_{eff} (Å)	λ_J (μm)
G4Fu	220±5	4.4±0.2	1.1±0.1	1150±120	317±18
G5Ed	240±5	4.6±0.2	2.8±0.1	917±92	226±11
G8Ed	250±5	5.0±0.2	7.8±0.4	n.a.	136±4

The microwave surface impedance of the $Nb_{.75}Zr_{.25}$ films was estimated from the current steps induced on the I-V characteristics, at finite voltages, in the presence of a suitable magnetic field. These current singularities (usually called Fiske steps) are described by the Kulik[17] theory of self-resonances in small junctions. We observed these steps in some samples. In Fig. 6 we show the I-V characteristic of sample G5Fd in a magnetic field H=0.24 gauss. The amplitude of the Fiske steps is mainly related to the surface impedance of the films[18,1], in a way that depends on the junction quality factor Q. In Fig. 7 the magnetic field behavior of the 1st and the 2nd current steps, I_1 and I_2, of the junction G4Fu at 4.2 K are reported together with the Josephson maximum current I_J. In Table II we list the voltages V_n corresponding to the maximum Fiske amplitude, the Josephson frequency $\nu_n = 2eV_n/h$, the speed of the electromagnetic field in the junction $\bar{c} = \nu_n\, 2L/n$, and the junction specific capacitance $C_s = \varepsilon_r \varepsilon_o / t$. The ratio ε_r/t is computed from $\bar{c}/c = (t/\varepsilon_r d)^{1/2}$.

TABLE II - Microwave properties of the junctions.

junction	n	V_n (μV)	ν_n (GHz)	$\bar{c}/c$ x10^{-2}	C_s (F/m^2)
G4Fu	1	18	9	1.3	0.22
G4Fu	2	36	18	1.3	0.22
G5Ed	1	16	8	1.3	0.29
G5Ed	2	32	16	1.3	0.29

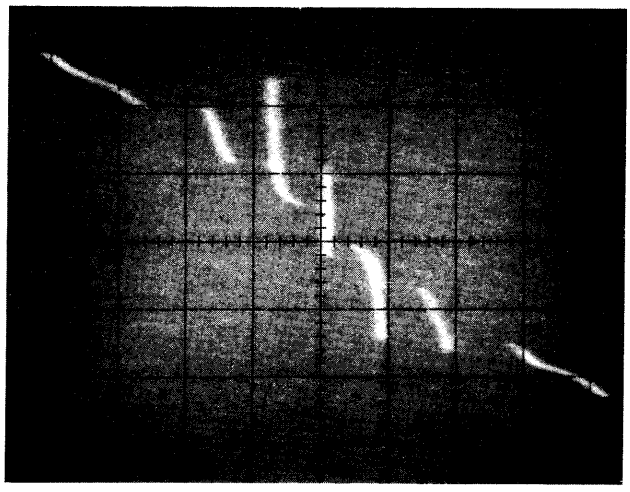

FIG. 6 - I - V characteristic of samples G5Fd in the presence of a magnetic field B=0.24 gauss. Horizontal scale 50 μV/div, vertical 500 μA/div.

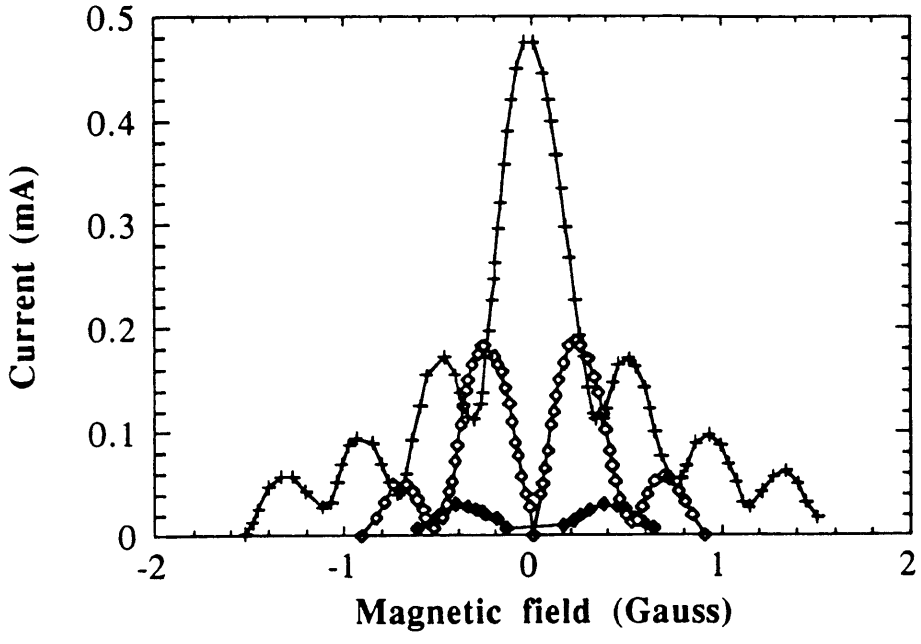

FIG. 7 - Magnetic behavior at 4.2 K of the maximum Josephson current (crosses), 1st Fiske step (open square), and 2nd fiske step (solid square) for the sample G4Fu

The theoretical dependence of the first self-induced resonance on the magnetic field, valid for small junctions with high Q, is given, in terms of the magnetic flux ϕ, by[19]:

$$I_1(\phi)=I_{c_o} J_o(\tfrac{a}{2})\, J_1(\tfrac{a}{2})\, F_1(\phi) \qquad (1)$$

where I_{co} is the maxiumum Josephson current, and J_o, J_1 respectively are the Bessel functions of zero and first order. The parameter a is the first solution of the implicit equation[20]:

$$J_o(\tfrac{a}{2}) = \sqrt{\frac{a}{Z_1 F_1(\phi)}} \qquad (2)$$

In this expression Z_1 is proportional to the junction quality factor and $F_1(\phi)$ is the Kulik function derived for the case of uniform Josephson current. From Eqs. (1) and (2) it comes out that the ratio $I_1^M/(I_{co}F_1(\phi))$ vs $Z_1F_1(\phi)$, where the superscript M indicates the maximum step amplitude, is an universal function[20] independent of ϕ. For t he sample G4Fu we found $I_1^M/(I_{co}F_1(\phi))$ $\approx$0.36, larger than the theoretical 0.34 computed with Eq. (1).

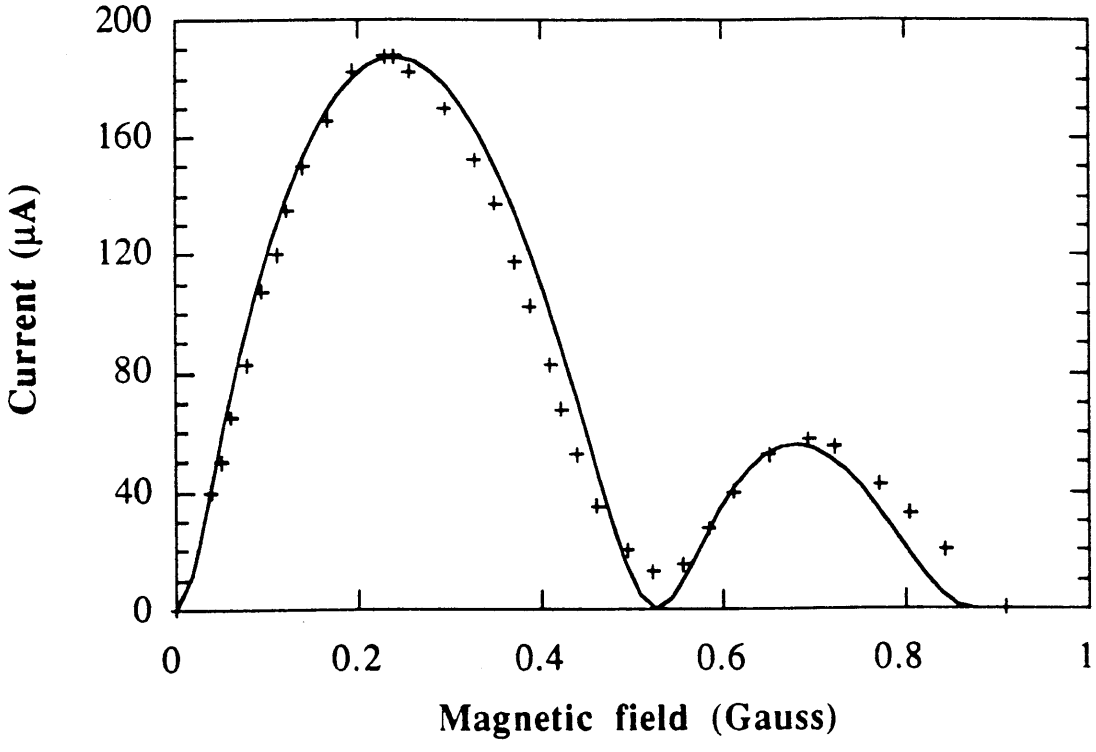

FIG. 8 - Theoretical dependance of the first self-resonance of a Josephson junction with Zn=6 on the applied magnetic field (solid line); crosses represent the experimental data reported in Fig. 7

Taking into account the asymmetrical current distribution in the junction, as previously considered, we computed the factor $F_1(\phi)$ with Eq. (10) of ref. 15 using again s_1=0.58 L and s_2=0.20 L. This resulted in a larger $F_1(\phi)$ and $I_1^M/(I_{co}F_1(\phi)) \approx 0.32$. The corresponding value of Z_1 on the universal curve is $\approx$6.

In Fig. 8 we show the experimental behavior of the first Fiske step for G4Fu; in the same

figure we plot Eq. (1) computed for Z_1=6. The agreement is satisfactory. Finally we compute the junction Q using:

$$Z_n = \left(\frac{L}{\lambda_j}\right)^2 \frac{Q_n}{\pi^2 n^2}$$

We find $Q_1 \approx 21$ for sample G4Fu at frequency $\nu_1 \approx 9$ GHz. The surface resistance is[18] $R_s = X_s/Q$, where $X_s = 2\pi\mu_o\lambda_{eff}\nu$ is the imaginary part of the surface impedance. We obtain $X_s \approx 7.8 \times 10^{-3}\ \Omega$ and finally $R_s = X_s/Q \approx 3.7 \times 10^{-4}\ \Omega$ at 4.2 K and ν=9 GHz. This results does not agree completely with the value $R_s = 1.4 \times 10^{-4}\ \Omega$ measured[9] on a $Nb_{.75}Zr_{.25}$ film at 4.2 K in a TE cavity at 7.8 GHz, even accounting for the frequency difference. We believe that the discrepancy may be mainly ascribed to the different techniques used for the measurement. The assumption that the losses are almost entirely due to the surface resistance are supported by the simple estimate of the second major contribution to the losses[18]: the quasiparticle tunneling losses Q_p. This term is evaluated by means of:

$$Q_p = 2\,\pi\,\nu_1\,R_d\,C_s\,W\,L$$

At the dynamical resistance corresponding to the step voltage, $R_d \approx 1.5\ \Omega$, we estimated $Q_p \approx 3000$. This value is two orders of magnitude above the one evaluated from the surface resistance.

5 - CONCLUSION

We have fabricated several symmetrical $Nb_{.75}Zr_{.25}$/Ox/$Nb_{.75}Zr_{.25}$ tunnel junctions by using thin film technology in order to investigate the superconducting properties of $Nb_{.75}Zr_{.25}$. Although our fabrication process was very simple the junctions showed tunneling characteristics useful for extensive gap measurements. The temperature behavior of the energy gap is in reasonable agreement with the BCS theory. Moreover by means of Josephson tunneling we have measured the magnetic penetration depth and the microwave surface resistance of $Nb_{.75}Zr_{.25}$ thin films.

ACKNOWLEDGEMENTS

The authors are indebted with Prof. R. Vaglio, University of Salerno, for helpful discussions and suggestions. We also appreciated the technical support of Mr. R. Ceccarelli and M. De Giorgi, Frascati National Laboratories.

REFERENCES

[1] A. M. Cucolo, A. Nigro, R. Vaglio, J. Low Temp. Phys. **69** 5/6, 363 (1987)

[2] C. Benvenuti, N. Circelli, M. Hauer, W. Weingarten, IEEE Trans. on Mag.**MAG 21** 2, 153 (1985)

[3] E. L. Wolf, R. J. Noer, Solid State Comm. **30**, 391 (1979)

[4] E. L. Wolf, R. J. Noer, G. B. Arnold, J. Low. Temp. Phys. **40** 5/6, 419 (1980)

[5] J. K. Hulm, R. D. Blaugher, Phys. Rev. **123** 5, 1569 (1961)

[6] H. J. Spitzer, J. Vac. Sci. Technol. **7** 5, 537 (1970)

[7] R. Delesclefs, Ø. Fischer, J. Low Temp. Phys. **53** 3/4, 339 (1983)

[8] I. Dietrich, Phys. Lett. **9** 3, 221 (1964)

[9] D. Di Gioacchino, P. Fabbricatore, S. Frigerio, U. Gambardella, R. Musenich, R. Parodi, G. Paternò, S. Rizzo, C. Vaccarezza, IEEE Trans. on Mag. **MAG-27** 2, 1299 (1991)

[10] I. Giaever, Phys. Rev. Lett. **5** 4, 147 (1960)

[11] J. Nicol, S. Shapiro, P. H. Smith, Phys. Rev. Lett. **5** 10, 461 (1960)

[12] G. B. Arnold, Phys. Rev. **B 18**, 1076 (1978)

[13] B. Muhlschlegel, Z. Physik **155**, 313 (1959)

[14] L. R. Testardi L. F. Mattheiss, Phys. Rev. Lett. **41** 23, 1612 (1978)

[15] G. Paterno', A. M. Cucolo, R. Vaglio, J.Appl. Phys. **60** 4, 1455 (1986)

[16] A. Barone and G. Paternò, Physics and Applications of the Josephson Effect (John Wiley & Sons, 1982) p. 70

[17] I. O. Kulik, Sov. Phys. - Tech. Phys., **12** 1, 111 (1967)

[18] T. C. Wang, R. I. Gayley, Phys. Rev. B **18** 1, 293 (1978)

[19] Y. S. Gou, R. I. Gayley, Phys. Rev. B **10** 11, 4584 (1974)

[20] A. Barone and G. Paternò, Physics and Applications of the Josephson Effect (John Wiley & Sons, 1982) p. 259